JOURNAL OF MATERIALS SCIENCE 26 (1991) 5575–5584

Si_3N_4 ceramics formed by HIP using different oxide additions – relation between microstructure and properties

E. M. KNUTSON-WEDEL, L. K. L. FALK, H. BJÖRKLUND
Department of Physics, Chalmers University of Technology, S-412 96 Göteborg, Sweden
T. EKSTRÖM
AB Sandvik Hard Materials, Box 420 56, S-126 12 Stockholm, Sweden

Si_3N_4-based ceramic materials formed by glass encapsulation and hot isostatic pressing (HIP) using different additions of Al_2O_3, Y_2O_3 and ZrO_2 have been characterized by analytical electron microscopy and X-ray diffractometry. The microstructures have been related to formation process and to room temperature hardness and fracture toughness of the ceramics. A high volume fraction of retained α-Si_3N_4 after processing at 1550 °C gave the Si_3N_4 ceramics high hardness. The equi-axed grain morphology of the Si_3N_4 matrices in these materials, which contained only small amounts of residual glass, resulted in comparatively low fracture toughness values. Processing at 1750 °C reduced the amount of retained α-Si_3N_4 substantially. When Y_2O_3 was added, the microstructure contained a comparatively large volume fraction of residual glass, and the Si_3N_4 was present mainly as high aspect ratio β-Si_3N_4 grains. This type of microstructure gave an Si_3N_4 ceramic material with high fracture toughness combined with a lower hardness. Additions of ZrO_2 and/or Al_2O_3 resulted also at 1750 °C in an extremely small volume fraction of residual glass, and a major part of the Si_3N_4 was present as equi-axed grains. These ceramics exhibited medium hardness and toughness values, however, larger additions of ZrO_2 appeared to slightly increase toughness.

1. Introduction

The compound Si_3N_4 has an extremely low self diffusivity due to the strongly covalent character of the Si–N bond. In order to obtain dense Si_3N_4 bodies by solidification of Si_3N_4 powder compacts, additions of metal oxide sintering aids are thus generally required. At the sintering temperature, the oxide additives react with the silica present on the Si_3N_4 powder particles and some of the Si_3N_4, and an oxynitride liquid phase is formed which acts as mass transport medium during densification [1–4]. Upon cooling, a residual intergranular glassy phase, and possibly also secondary crystalline phases, will form from the liquid [3, 5]. These phases often degrade mechanical properties, particularly at elevated temperatures, and may also have a detrimental effect on the oxidation resistance of the ceramic [3, 5–8]. It is hence of considerable interest to form Si_3N_4 ceramics with a minimum of metal oxide additives. The development of glass encapsulation followed by hot isostatic pressing (HIP) has enabled the formation of fully dense Si_3N_4 bodies using only small amounts of sintering aids [9].

Si_3N_4-based ceramic materials have a high potential for a number of structural applications with different requirements on mechanical and chemical properties. As an example, some types of Si_3N_4-based ceramics have been successfully employed as cutting tools for machining of aerospace alloys and cast iron [10, 11]. This is an application where a relatively high fracture toughness of the ceramic is required. A high hardness is, on the other hand, desirable in applications like sealing devices and blast nozzles.

Recent work on Si_3N_4-based ceramics formed by HIP has shown that it is possible to control room temperature mechanical properties, such as hardness and fracture toughness, via parameters in the formation process, Fig. 1 [12]. It was established that type and amount of oxide sintering additive, as well as time and temperature of HIP, played an important role in determining the performance of the ceramic material. Primarily, various small amounts of Y_2O_3, Al_2O_3 and ZrO_2 were added to the Si_3N_4 ceramics, but it was also found that larger additions of oxide sintering aids, particularly ZrO_2, could indeed be used to give the ceramic a favourable combination of hardness and toughness [12].

The present paper concerns a microstructural characterization of the different Si_3N_4-based ceramics in the hardness–fracture toughness diagram in Fig. 1. Special attention has been given to the relation

0022–2461/91 $03.00 + .12

between fabrication process and microstructure, as well as to how resulting microstructure affects the properties of the ceramic.

2. Experimental procedure

The Si_3N_4 ceramics were formed by glass encapsulation followed by HIP at a pressure of 200 MPa. Three different processing conditions were employed: 2 h at 1550 °C, 1 h at 1750 °C and 2 h at 1750 °C. Table I gives the different compositions of the Si_3N_4 ceramics which were prepared in the present investigation. The Si_3N_4 starting powder was H. C. Starck-Berlin, LC1, which contains 94–95% α-Si_3N_4 and has an oxygen content which corresponds to 2.9 wt % surface SiO_2. The different oxide additives were ZrO_2(Chema Tex, SC16), ZrO_2 stabilized with 3 mol % Y_2O_3 (TOSOH, TZ-3Y), Al_2O_3 (Alcoa, A16SG) and Y_2O_3 (H. C. Starck, Finest). A detailed description of the preHIP processing is given by Ekström *et al.* [12].

Microstructural characterization was carried out by X-ray diffractometry and analytical electron microscopy using scanning and transmission microscopy (SEM, TEM, STEM) with energy dispersive X-ray analysis (EDX). Specimens for SEM were prepared by diamond polishing followed by plasma etching using CF_4 gas. This technique removes, preferentially, grains of Si_3N_4 and Si_2N_2O which leaves a network containing the grain boundary phases. A CamScan S4-80DV scanning electron microscope was used for analysis. Thin foils for TEM and STEM were prepared from 0.5 mm thin slices cut by a high speed diamond saw. These slices were ground, diamond polished and ion beam milled to electron transparency. The thin foils were investigated in a Jeol 2000-FX TEM/STEM/SEM instrument with an attached Link EDX system for quantitative elemental analysis. In order to avoid charging in the electron microscope all samples were coated with a thin evaporated carbon film.

Phase compositions were determined by X-ray diffractometry of polished sections. The relative amount

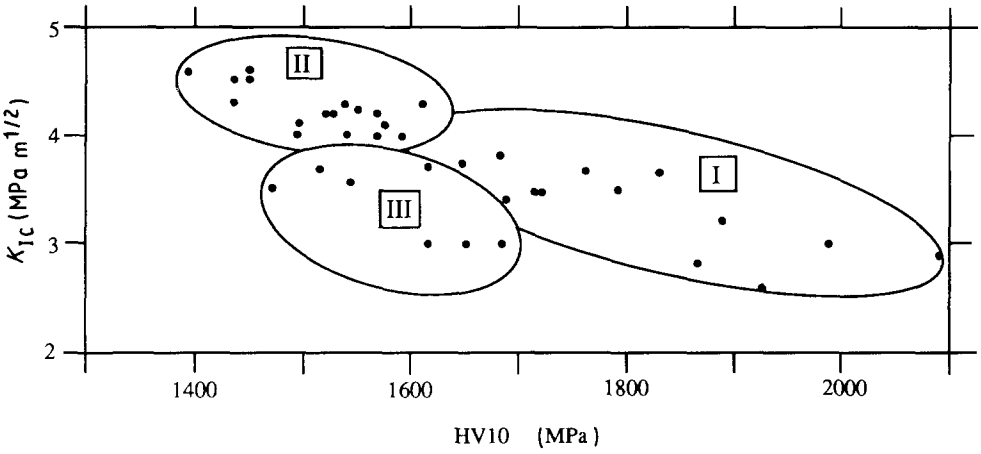

Figure 1 Hardness and fracture toughness of the Si_3N_4 based materials in the present investigation. Three different classes of materials, I, II, and III, with different mechanical properties could be identified.

TABLE I Oxide additions (in wt %) and processing conditions given together with phase compositions of the Si_3N_4 ceramics in the present investigation

Al_2O_3	Y_2O_3	ZrO_2	1550 °C, 2 h	1750 °C, 1 h	1750 °C, 2 h
2	/	/	α, β, S	α, β, S	α, β, S
/	2	/	α, β, p	α, β, S	β, S
2	2	/	α, β, S	α, β, S	β, S
2	/	2	α, β, t	α, β, S, t	α, β, S, t
/	2	10	α, β, S, t, p	β, S, t	
2	2	10	α, β, S, t	β, S, t	
/	/	20[a]	α, β, S, t, p	β, S, t	
2	/	20[a]	α, β, t	β, S, t	
/	4	/	α, β, S, p	α, β, S	
2	4	/	α, β, S	β, S	
4	4	/	α, β, S	β, S	
4	2	/	α, β, S	α, β, S	
4	6	/	α, β	α, β	
/	2	5[a]	α, β, S, t, p	α, β, S, t	
/	2	5	α, β, S, t, p	β, S, t	
2	/	5[a]	α, β, S, t	β, S, t	
2	/	5	α, β, S, m, t	β, S, m, t	
/	6	/		α, β	

α: α-Si_3N_4, β: β-Si_3N_4, S: Si_2N_2O, m, t: monoclinic, tetragonal ZrO_2, p: porous, [a] prereacted with 3 mol % Y_2O_3.

of retained α-Si_3N_4 after processing, referred to as the Q-value, was determined by peak intensity ratios, $\alpha/(\alpha + \beta)$, from X-ray diffractograms. In these calculations, integrated intensities of the (1 0 2) and (2 1 0) peaks from the α phase and the (1 0 1) and (2 1 0) peaks from the β phase were used. The crystal structure of the ZrO_2 grains in materials formed with additions of ZrO_2 powder was determined in a similar way by T, which is the peak height ratio tetragonal–(tetragonal + monoclinic). Integrated intensities from the tetragonal (1 1 1) and (2 0 2) and the monoclinic (1 1 1) and (1 1 - 1) reflections were used for calculation of T. A detailed discussion of the X-ray diffractometry analysis is given in reference [12].

A possible incorporation of Al and O into the β-Si_3N_4 lattice during densification of the Al_2O_3 containing Si_3N_4 ceramics was estimated by the z value in the β sialon formula, $Si_{6-z}Al_zO_zN_{8-z}$. The z values were determined from Al–Si ratios obtained by EDX in STEM of individual β-Si_3N_4 grains.

3. Results

3.1. The general microstructure of the Si_3N_4 ceramics

The general microstructure of the different Si_3N_4-based ceramics consisted of α- and β-Si_3N_4, Si_2N_2O and a residual intergranular glassy phase, see Table I. When ZrO_2 powder was added to the starting powder mixture, the ceramic also contained grains of ZrO_2. The volume fractions of the different phases were strongly dependent upon both composition and process, i.e. time and temperature of HIP. As indicated in Table I, some of the compositions did not result in fully dense bodies.

With respect to the morphology of the Si_3N_4 grains and the intergranular microstructure, the samples could schematically be divided into three groups which in the following will be denoted A, B and C. Group A contains all samples HIPed for 2 h at 1550 °C. The Si_3N_4 grains in these microstructures had in general an irregular shape, and were separated by a comparatively low volume fraction of residual glass, Figs 2 and 3. This glass was concentrated to comparatively small pockets adjacent to smaller, often faceted, Si_3N_4 grains, Fig. 3. X-ray diffractometry showed that the Q value varied between 0.56 and 0.86, Fig. 4; thus a significant volume fraction of the α-Si_3N_4 had not transformed to the β structure. Materials formed without an addition of Al_2O_3 did not achieve full density at 1550 °C, see Table I and Fig. 2b.

Group B contains samples densified at 1750 °C with a separate addition of Y_2O_3. These materials contained the highest volume fraction of residual glass, and the glassy phase was present as thin intergranular films merging into pockets at multigrain junctions, Figs 2c, 5 and 6. EDX analysis of a number of larger glass pockets (> 100 nm) showed that the residual glassy phase contained varying amounts of cations from the sintering aids, i.e. the composition of the glass

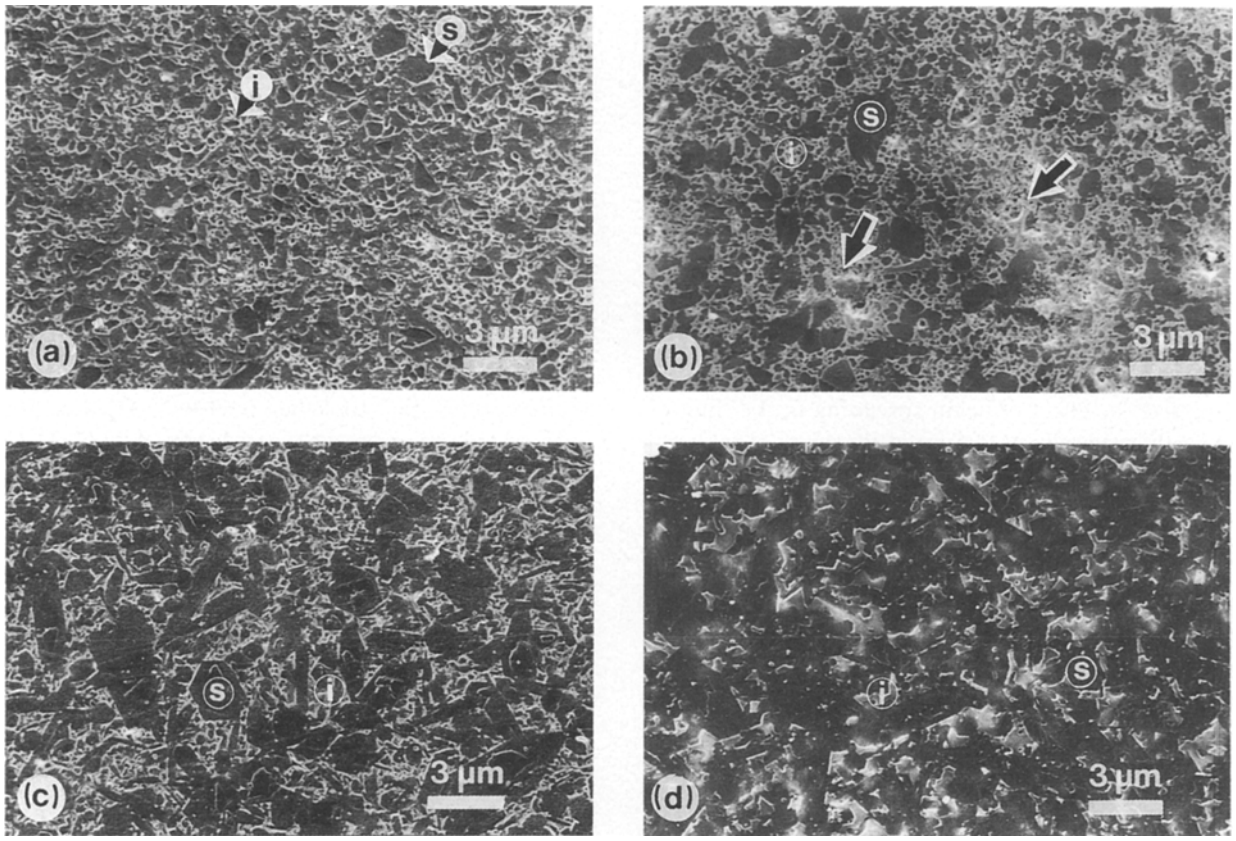

Figure 2 SEM micrographs of plasma etched surfaces. The Si_3N_4 and Si_2N_2O grains (s) have been preferentially etched leaving a network containing the intergranular phases (i). (a) HIP for 2 h at 1550 °C with additions of 2 wt % Y_2O_3 together with 2 wt % Al_2O_3. (b) HIP at 1550 °C with an addition of 4 wt % Y_2O_3. Pores (arrowed) are seen on the surface. (c) HIP for 1 h at 1750 °C with an addition of 4 wt % Y_2O_3 together with 4 wt % Al_2O_3. (d) HIP for 1 h at 1750 °C with an addition of 20 wt % ZrO_2 prereacted with 3 mol % Y_2O_3.

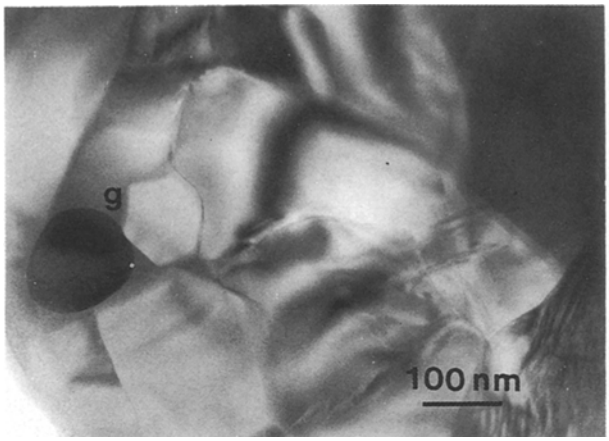

Figure 3 Bright field TEM micrograph of a material HIPed 2 h at 1550 °C with addition of 2 wt % Y_2O_3, 2 wt % Al_2O_3 and 10 wt % ZrO_2. The small volume fraction of residual glass was concentrated to smaller pockets (g) in the microstructure.

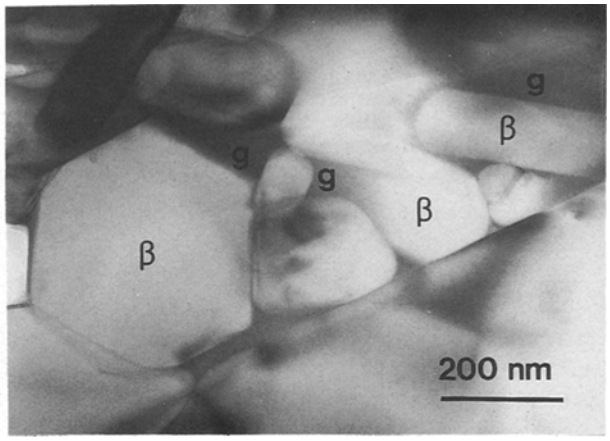

Figure 5 Bright field TEM micrograph showing faceted β-Si_3N_4 grains (β) separated by glassy pockets (g) in a ceramic HIPed 2 h at 1750 °C with an addition of 2 wt % Al_2O_3 together with 2 wt % Y_2O_3.

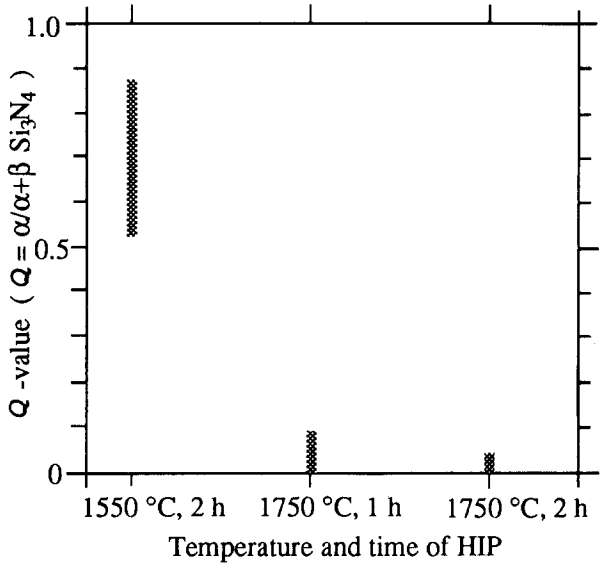

Figure 4 The relative amount of retained α-Si_3N_4, denoted Q, present in the different ceramics as function of processing conditions.

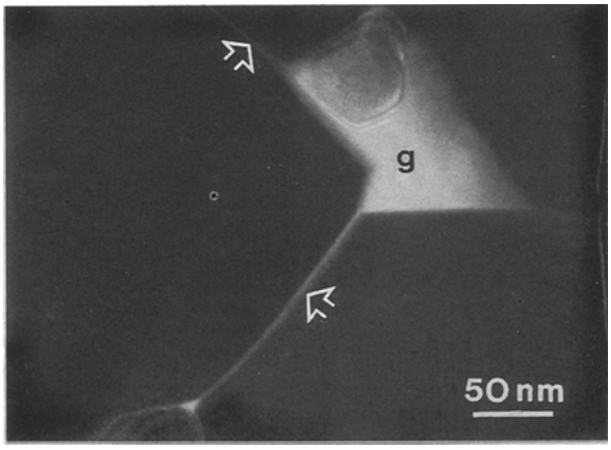

Figure 6 Centred dark field TEM micrograph formed using diffuse scattered electrons showing the presence of thin glassy grain boundary films (arrowed) merging into glass pockets at multi grain junctions (g). The ceramic was HIPed 1 h at 1750 °C with an addition of 2 wt % Al_2O_3 together with 2 wt % Y_2O_3.

was not homogeneous throughout the microstructure. Only larger glass pockets were analysed in order to minimize the effect of beam spreading in the thin foil. One other significant feature of this class of materials was that the majority of the β-Si_3N_4 grains had a faceted cross-section and a relatively high aspect ratio, Figs 2c and 5.

Group C contains samples HIPed at 1750 °C without the separate Y_2O_3 addition. These ceramics had an extremely low volume fraction of residual glass, Fig. 7. Only very thin glassy films separating adjacent grains could be detected in the TEM by centred dark field imaging using diffuse scattered electrons or by a defocusing method described by Clarke [13]. In these Si_3N_4 ceramics formed without the separate Y_2O_3 addition, the shape of a majority of the β-Si_3N_4 grains became close to equiaxed, Fig. 8. When Y_2O_3 stabilized ZrO_2 powder was added, however, an increased fraction of the β grains exhibited a higher aspect ratio, Fig. 9.

A majority of the samples in this investigation contained Si_2N_2O present mainly as larger, elongated, faulted grains, Fig. 10. When 6 wt % Y_2O_3 was, however, added separately or together with 4 wt % Al_2O_3, Si_2N_2O did not form at any of the two densification temperatures 1550 and 1750 °C. At 1550 °C, three other compositions did also preclude Si_2N_2O from the microstructure, namely Si_3N_4 with additions of 2 wt % Y_2O_3, 2 wt % Al_2O_3 together with 2 wt % ZrO_2 and 2 wt % Al_2O_3 together with 20 wt % ZrO_2 stabilized with 3 mol % Y_2O_3, see Table I.

3.2. α/(α + β) Si_3N_4 ratio in ceramics formed with Y_2O_3 and Al_2O_3

Ceramics densified at 1750 °C contained a reduced amount of retained α-Si_3N_4. The Q values for the ceramics in groups B and C were determined to be between zero and 0.08, Figs 4 and 11a. A prolonged holding time at the densification temperature 1750 °C

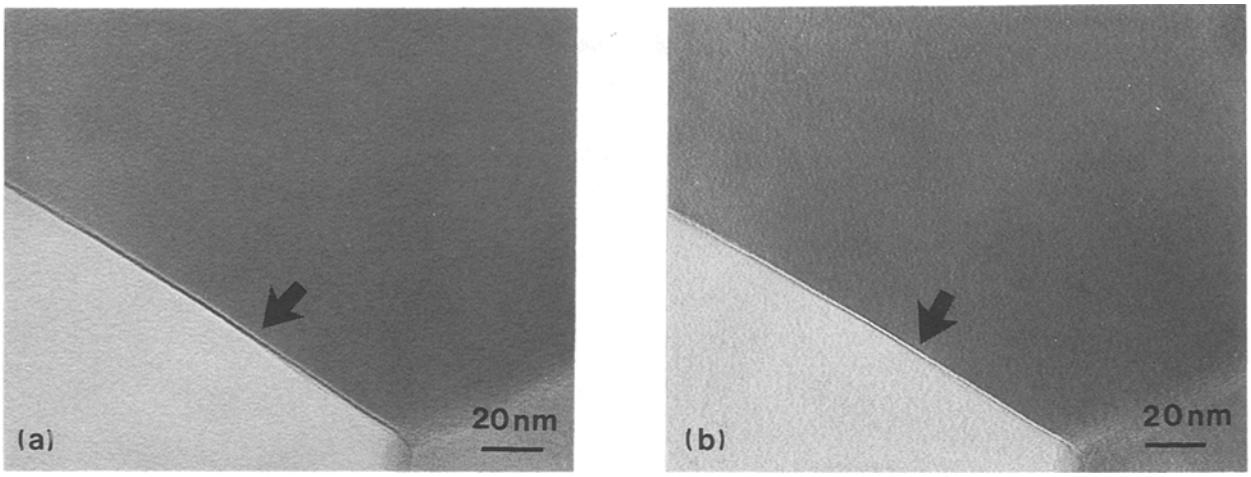

Figure 7 Bright field TEM micrograph of a grain boundary in a ceramic densified 2 h at 1750 °C with an addition of 2 wt % Al_2O_3. (a) Overfocused image, (b) underfocused image. The fringe contrast (arrowed) shows the presence of a thin intergranular film [13].

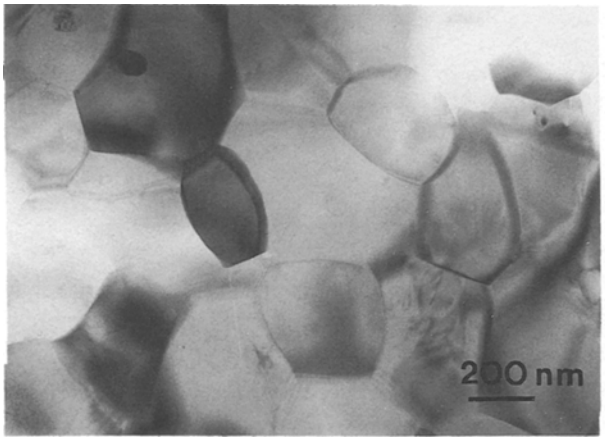

Figure 8 Bright field TEM image showing the equiaxed grain morphology in a ceramic densified 1 h at 1750 °C with an addition of 2 wt % Al_2O_3.

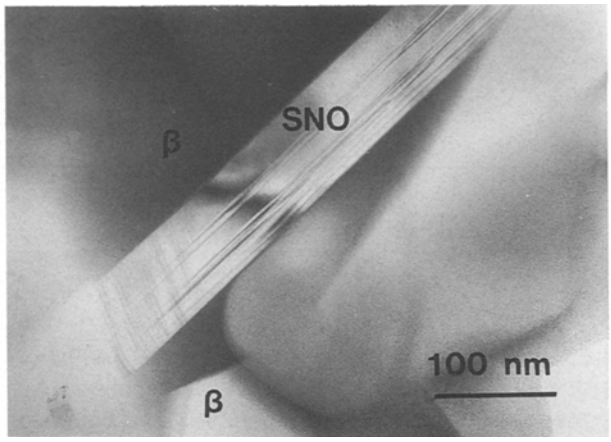

Figure 10 Bright field TEM image of material densified 1 h at 1750 °C with an addition of 2 wt % Y_2O_3. An Si_2N_2O grain (SNO), which is heavily faulted, is located adjacent to β-Si_3N_4 grains (β).

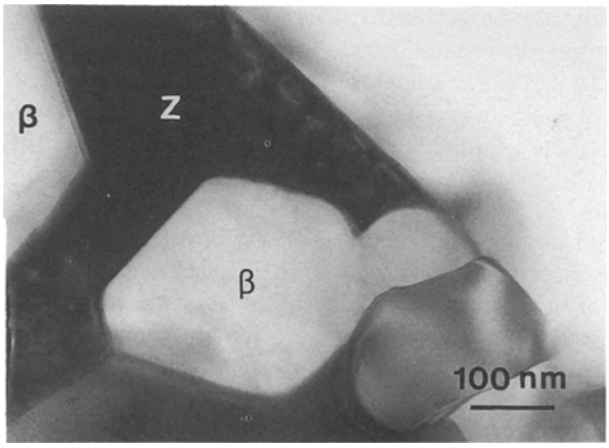

Figure 9 Bright field TEM micrograph of material HIPed for 1 h at 1750 °C with an addition of 20 wt % ZrO_2 prereacted with 3 mol % Y_2O_3. Elongated and faceted β-Si_3N_4 grains (β) are surrounded by grains of ZrO_2 (z), which have highly irregular shapes.

resulted in a further transformation of α to β-Si_3N_4 and this seemed to be promoted by small additions of Y_2O_3(2 wt %), Fig. 11c.

The diagrams in Figs 11a and b indicate that when the relative Y_2O_3 and Al_2O_3 contents exceeded some critical values, the amount of unreacted α-Si_3N_4 in the HIPed ceramic increased. This is clearly demonstrated in Fig. 11a, where it can be seen that for a certain Al_2O_3 addition, there is a minimum in Q for an Y_2O_3 content of 4 wt % after densification at 1750 °C, 1 h. A similar behaviour is observed for materials formed with 2 wt % Y_2O_3 and varying amounts of Al_2O_3, Fig. 11a.

3.3. Si_3N_4 ceramics formed with ZrO_2

In materials formed with additions of ZrO_2 or ZrO_2-(+ 3 mol % Y_2O_3) powder and densified at 1750 °C, the α to β Si_3N_4 transformation was complete in most samples. Only in three materials could small amounts of retained α be detected by X-ray diffractometry, see Table I. Addition of 2 wt % ZrO_2 together with 2 wt % Al_2O_3 resulted in a Q value of 0.03 after 1 h and 0.01 after 2 h, and 5 wt % ZrO_2 (+ 3 mol % Y_2O_3) added together with 2 wt % Y_2O_3 gave $Q = 0.05$ after 1 h at this temperature.

The ZrO_2 was present either as grains with highly irregular shape filling out space between grains of Si_3N_4 and Si_2N_2O, or as small equiaxed grains, Figs

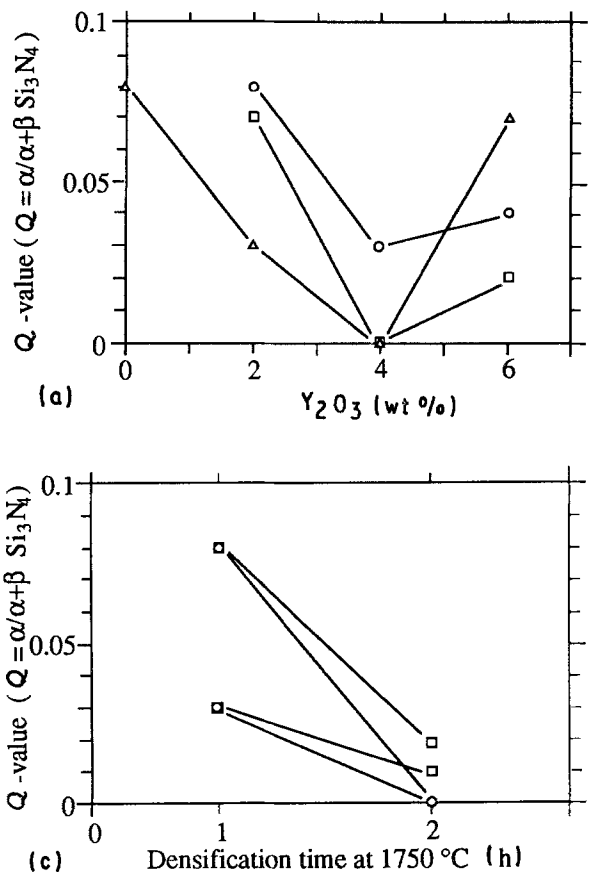

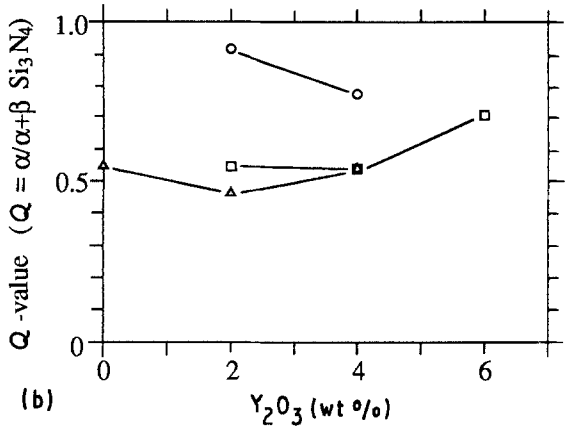

Figure 11 The relative amount of retained α-Si_3N_4 (Q) as function of Y_2O_3 addition after HIP at (a) 1750 °C (○ 0 wt % Al_2O_3, △ 2 wt % Al_2O_3, □ 4 wt % Al_2O_3) and (b) 1550 °C (○ 0 wt % Al_2O_3, △ 2 wt % Al_2O_3, □ 4 wt % Al_2O_3). In (c) (○ with Y_2O_3 addition, □ without Y_2O_3 addition), Q is displayed as function of time at 1750 °C.

2d and 9. As shown in Table I, only one composition, the addition of 5 wt % unstabilized ZrO_2 together with 2 wt % Al_2O_3, resulted in detectable amounts of monoclinic ZrO_2 in the microstructure. This composition gave a T value of 0.41 after densification at 1550 °C, and a slightly higher value, 0.52, i.e. a smaller fraction monoclinic phase, after HIP at 1750 °C.

When the Y_2O_3 and the ZrO_2 were added separately, it was shown by EDX in the STEM that a significant part of the Y_2O_3 was incorporated into the ZrO_2 grains during densification. The glassy phase in these ceramics contained, apart from other cations, both Y and Zr. The ZrO_2 phase in Si_3N_4 ceramics formed with the Y_2O_3 stabilized ZrO_2 powder retained the Y_2O_3 in the densified body. These ceramics had, as described in Section 3.1, an extremely small volume fraction of residual glass.

3.4. Incorporation of Al and O into the β-Si_3N_4 grains

When Al_2O_3 was added, EDX in the STEM showed that Al was dissolved in the β-Si_3N_4 grains which formed during densification. A detailed investigation of samples formed at 1750 °C and with 2 wt % Al_2O_3, alone or together with other oxide additives, showed that 2 to 3 wt % Al, with respect to the Si and Al content, was dissolved in the β structure. This corresponds to z values between 0.13 and 0.18 in the β sialon formula $Si_{6-z}Al_zO_zN_{8-z}$. Similar results were obtained by lattice parameter refinements of X-ray diffractograms as reported by Ekström *et al.* [12]. When the Al_2O_3 was added together with Y_2O_3, the results from X-ray diffractometry gave $z = 0$ although EDX showed the presence of small amounts of Al in a number of the analysed β-Si_3N_4 grains.

4. Discussion

4.1. Development of microstructure

4.1.1. Densification process

The densification process is in general described by the three successive stages of Kingery's model for liquid phase sintering [14], namely particle rearrangement, solution of α-Si_3N_4 followed by precipitation of β-Si_3N_4 and coalescence. The requirements on the liquid phase sintering medium are that there is a sufficient volume fraction of liquid phase which exhibits complete wetting of the solid phase, and that the solid phase has an appreciable solubility in the liquid. During consolidation by HIP, the applied high pressure promotes densification significantly, and equilibrium may not be attained in the solution–reprecipitation process before full density is achieved. This will result in a certain amount of retained α-Si_3N_4 in the fully dense ceramic. The present investigation has shown that the volume fraction of retained α-Si_3N_4 in HIPed Si_3N_4-based materials is dependent not only upon time and temperature of HIP, but also upon type and amount of sintering aids as will be discussed in Section 4.1.2 below.

The metal oxide sintering additives will determine the eutectic temperature and also the volume fraction and viscosity of the liquid phase which forms during densification. The additives used in this work give eutectic temperatures in the range 1345 to 2380 °C in the pure oxide systems, see Table II, but it has been indicated that the presence of N lowers these eutectic temperatures further [1, 24]. Eutectic temperatures of 1470, 1480 and 1590 °C have been reported in the SiO_2–Al_2O_3–Si_3N_4, SiO_2–Y_2O_3–Si_3N_4 and the SiO_2–ZrO_2–Si_3N_4 systems, respectively [23]. Furthermore, impurities introduced during powder processing will also decrease the eutectic temperature. This implies, that due to the presence of a larger volume fraction liquid phase, Si_3N_4 ceramics formed

TABLE II Eutectic temperatures of relevant oxide systems

Oxides	Eutectic temperature (°C)	Reference
SiO_2	1726[a]	[15]
SiO_2–Al_2O_3	1595	[16]
SiO_2–Y_2O_3	1660	[17]
SiO_2–ZrO_2	1640	[1]
SiO_2–Al_2O_3–Y_2O_3	1345	[18]
SiO_2–Al_2O_3–ZrO_2	1539 (calculated)	[19]
Al_2O_3–Y_2O_3	1760	[20]
Al_2O_3–ZrO_2	1710	[21]
Y_2O_3–ZrO_2	2380	[22]
SiO_2–Y_2O_3–Si_3N_4	1470	[23]
SiO_2–Al_2O_3–Si_3N_4	1480	[23]
SiO_2–ZrO_2–Si_3N_4	1590	[23]

[a] melting temperature

with appropriate additions of Y_2O_3 together with Al_2O_3, or ZrO_2 together with Al_2O_3, would densify more easily at lower temperatures than ceramics formed with one single oxide additive. That has also been found for pressureless sintering of Si_3N_4 ceramics formed with Y_2O_3, where, generally, small additions of Al_2O_3 are used to lower the eutectic temperature during densification [4].

Despite the applied high pressure, dense Si_3N_4 bodies were not obtained at 1550 °C using only a small addition of Y_2O_3 or Y_2O_3 together with ZrO_2, see Table I. This was also the case when 20 wt % ZrO_2 powder stabilized with 3 mol % Y_2O_3 was added; this material was extremely porous. When Al_2O_3 was added, however, a single addition of only 2 wt % resulted in full densification under the same processing conditions. From the discussion above, it can be concluded that the volume fraction of liquid phase in compacts formed without Al_2O_3 was comparatively low at 1550 °C, and thus full densification could not be achieved. At 1750 °C however, the volume fraction of liquid phase will increase which is in accordance with the formation of fully dense bodies and the observation of larger volume fractions of residual glass in a number of the compacts densified at this temperature.

The presence of Y, as well as an increased concentration of N, in the oxynitride liquids which form in these systems is known to increase the viscosity of the liquid, and that will also affect the densification process [1, 25]. An increased viscosity of the liquid phase sintering medium will reduce the shrinkage rate during the particle rearrangement stage and also reduce the material transport through the liquid so that the α to β Si_3N_4 transformation occurs without much contribution to the shrinkage of the compact [1]. This may also contribute to the porous nature of compacts formed with Y_2O_3 but without Al_2O_3 at 1550 °C.

4.1.2. $\alpha/(\alpha+\beta)$ Si_3N_4 ratio

There was a general reduction in the amount of retained α-Si_3N_4 in the ceramic after processing at 1750 °C, Fig. 4. Since the α- to β-Si_3N_4 transformation takes place via the liquid phase sintering medium, this may be explained by the increased volume fraction of liquid at the higher temperature as well as an increased solubility and ion mobility in the liquid. This would also be affected by the particular metal oxide sintering aids, and as indicated in Table I and Fig. 11, certain oxide additives, and combination of additives, promoted the α to β transformation. Table I indicates that larger additions of ZrO_2 in combination with smaller additions of the other oxides always resulted in a sufficient volume fraction of liquid phase sintering medium at 1750 °C which assured a complete α to β transformation and full densification. The increase in volume fraction of retained α-Si_3N_4 with increasing Y_2O_3 or Al_2O_3 addition in ceramics formed without ZrO_2, Fig. 11, was possibly caused by a shift of the composition between compatibility triangles. In the pure oxide system, the lowest eutectic temperature within a compatibility triangle increases with a relative reduction in the SiO_2 content [18].

A number of samples achieved full density before the α to β transformation was complete, Table I. Samples formed at 1750 °C and with additions of 2 wt % of the different oxides Y_2O_3, Al_2O_3 and ZrO_2 showed, however, that the transformation continued in the fully dense body, Fig. 11c. The Q values in the diagram in Fig. 11c suggest that the presence of small additions of Y_2O_3 promoted transformation, since material formed with 2 wt % Al_2O_3 or 2 wt % Al_2O_3 in combination with 2 wt % ZrO_2 still contained small amounts of retained α-Si_3N_4 after 2 h at 1750 °C.

4.1.3. Grain boundary phases and grain morphology

Materials densified at 1550 °C did not show any pronounced variations in the morphology of the Si_3N_4 and of the intergranular regions. During processing at 1750 °C, however, significant differences in the microstructures of the ceramics developed as described in Section 3.

In materials formed with a single addition of Y_2O_3 at 1750 °C, a majority of the β-Si_3N_4 grains had a faceted cross-section and a relatively high aspect ratio which imply that they had grown in an isotropic liquid phase environment [26]. This was also indicated by the comparatively large volume fractions of residual glass in these materials. The presence of Y_2O_3 from stabilized ZrO_2 powder did also promote the development of high aspect ratio β grains. As discussed in Section 4.1.4 below, it can be concluded that the ZrO_2 did participate in a liquid phase formation but only a limited fraction of the liquid phase present in the compact during densification was retained at room temperature in the form of a residual glassy phase.

When only Al_2O_3 was added, or Al_2O_3 together with ZrO_2, the amount of residual glass was extremely low, and the morphology of the Si_3N_4 grains was close to equiaxed. This significantly different morphology of the Si_3N_4 grains, as well as the absence of larger glass volumes in these materials, imply that the volume

fraction of liquid phase was reduced considerably during processing. EDX in the STEM showed that a considerable portion of the Al was incorporated into the β grains during densification, and this was combined with a formation of a secondary crystalline ZrO_2 phase in materials formed with additions of ZrO_2 powder. These processes would consume the constituents of the liquid, and hence reduce the volume of the liquid phase sintering medium as well as alter its composition. The composition of the remainder of the liquid would thus approach the Si_3N_4–SiO_2 border of the Si_3N_4–SiO_2–Al_2O_3–AlN behaviour diagram. This is also indicated by the presence of Si_2N_2O, which suggests that the remaining liquid had a composition close to Si_2N_2O. This behaviour is similar to what has been observed in the two-phase YAG-sialons which are reported to be virtually glass free after a suitable post-sintering heat treatment [27].

Some of the materials formed at 1550 °C did not contain Si_2N_2O although that phase formed when compacts with the same composition were HIPed at 1750 °C. This indicates that the liquid phase which formed at the lower temperature had a composition which did not favour the formation of Si_2N_2O. Larger additions of Y_2O_3 (6 wt %), even in combination with an Al_2O_3 addition, resulted both at 1550 and 1750 °C in a Y- and Al-rich liquid phase which was stable against formation of Si_2N_2O.

4.1.4. The ZrO_2 phase

It has been proposed previously that the ZrO_2 undergoes a solution–reprecipitation process in these systems during densification [28–30]. This is suggested also by the morphology of the ZrO_2 grains and the intergranular microstructure in the Si_3N_4–ZrO_2 ceramics in the present investigation. As discussed above, the formation of a crystalline ZrO_2 phase from the liquid during densification would reduce the volume fraction of the liquid phase sintering medium, hence result in a microstructure with a lower volume fraction of residual glass. It has, however, been indicated in previous work that the presence of stabilizing oxides such as Y_2O_3, added either in the form of doped ZrO_2 powder or separately, will have an influence on the amount of residual glass [28, 31]. This is confirmed by the present investigation; ceramics formed with ZrO_2 contained an increased volume fraction of residual glass, rich in Y and Zr, when Y_2O_3 was separately added.

The presence of Y_2O_3 resulted in all cases in a stabilization of the high temperature tetragonal ZrO_2 structure to room temperature. The T values for Si_3N_4–ZrO_2 ceramics formed without Y_2O_3 showed that a portion of the ZrO_2 phase was tetragonal also in these materials. The tetragonal structure of a ZrO_2 grain may be retained to room temperature by mechanical constraints imposed by the surrounding matrix. It cannot, however, be precluded that N had entered the ZrO_2 structure during densification, which might contribute to a stabilization of the tetragonal form [29, 31].

4.2. Relation between microstructure and mechanical properties

A characterization of room temperature hardness and fracture toughness of the Si_3N_4 ceramics in this investigation has been presented by Ekström *et al.* [12]. The hardness was determined by Vickers indentation using a 10 kg load, and fracture toughness was calculated from the indentation marks according to the method of Anstis [32]

$$K_{IC} = 1.6 \times 10^{-2} (E/H)^{1/2} P/(c_0)^{3/2}$$

where E is the modulus of elasticity (GPa), H = HV10 × 0.0981 (GPa), P the indentation load (N) and c_0 the impression radius + indentation crack length/4.

The so obtained values of mechanical properties divided the ceramics into three different classes, I, II and III, as shown in Fig. 1. Class I contains materials with a high hardness combined with a relatively low fracture toughness. Materials with a high fracture toughness but a reduced hardness form class II, and materials with intermediate hardness and toughness are denoted class III. The microstructural characterization showed that the materials also could be divided into three different groups with respect to their microstructures, and these groups were denoted A, B and C.

The temperature of HIP had a critical influence on room temperature mechanical properties, Fig. 12. When increasing the densification temperature from 1550 °C (group A) to 1750 °C (groups B and C) the hardness decreased and the fracture toughness increased significantly.

It has been proposed previously that the hardness of the α-Si_3N_4 is higher than that of the β phase [33]. It has also been suggested that a higher volume fraction of residual glass would reduce the hardness of the ceramic [34]. The results from the present investigation lend support to this; decreased Q values as well as larger volumes of glass were observed in the materials with low hardness.

The fracture toughness of materials densified at 1750 °C was clearly dependent upon the morphology of the Si_3N_4 grains which was determined by type and amount of oxide additives. Materials formed with a separate addition of Y_2O_3, group B, showed comparatively high values of fracture toughness, Fig. 1. This could be explained by the presence of high aspect ratio β-Si_3N_4 grains which may act as crack deflectors [35]. When Al_2O_3 was added, separately or together with ZrO_2, the equiaxed morphology of the Si_3N_4 was reflected in the reduced fracture toughness. A clear increase in fracture toughness was, however, observed for materials formed with larger additions of ZrO_2 [12].

The observed significant differences in microstructures between specimens in the three groups A, B and C are thus reflected in the mechanical properties. The groups A, B and C do correspond to the classes I, II and III, respectively, of mechanical properties with only one major exception; a larger addition of ZrO_2 raised the fracture toughness to a value higher than one would expect for a ceramic with that particular morphology of the Si_3N_4 matrix. Possible toughening

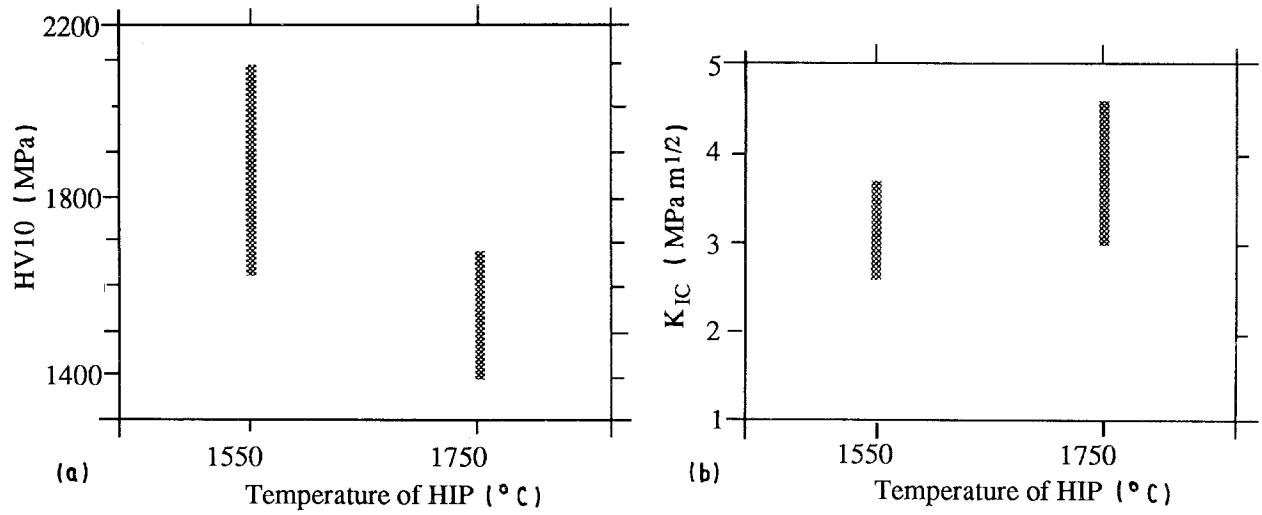

Figure 12 (a) Hardness and (b) fracture toughness as functions of processing conditions.

mechanisms are particle strengthening and, because of the tetragonal structure of the ZrO_2 grains, transformation toughening and ferroelasticity [36, 37].

5. Conclusions

The conclusions are as follows:

1. Time and temperature of HIP as well as type and amount of oxide sintering aid had a conclusive influence on microstructure and mechanical properties of the Si_3N_4 ceramics.
2. Small quantities of Al_2O_3 promoted densification significantly at 1550 °C.
3. HIP at 1550 °C resulted in Si_3N_4 grains with equiaxed shape which were separated by a comparatively low volume fraction of residual glass located to smaller pockets in the microstructure. A large amount of retained α-Si_3N_4 gave these materials a high hardness, while the grain morphology resulted in a relatively low fracture toughness.
4. HIP at 1750 °C reduced the volume fraction retained α-Si_3N_4 substantially. This lead to a simultaneous reduction in hardness.
5. HIP at 1750 °C with separate additions of Y_2O_3 resulted in a large volume fraction of residual glass present as thin intergranular films merging into pockets at multi grain junctions. High aspect ratio β-Si_3N_4 grains developed in these materials which resulted in a high fracture toughness.
6. HIP at 1750 °C without a separate addition of Y_2O_3 resulted in an extremely low volume fraction of residual glass present as very thin films separating adjacent grains. The shape of the β-Si_3N_4 grains were in general close to equiaxed, but when Y_2O_3 stabilized ZrO_2 powder was added, an increased fraction of the β grains exhibited a faceted cross section and a higher aspect ratio.
7. Larger additions of ZrO_2 increased the fracture toughness to a value higher than expected from the particular morphology of the Si_3N_4 matrix.

Acknowledgements

This project was supported by the Swedish National Board for Technical Development (STU) and AB Sandvik Hard Materials.

References

1. S. HAMPSHIRE and K. H. JACK, in "Special Ceramics 7", edited by D. Taylor and P. Popper (British Ceramic Research Association, Stoke-on-Trent, 1981) pp. 37–49.
2. F. F. LANGE, in "Nitrogen Ceramics", edited by F. L. Riley (Noordhoff, Leyden, 1977) pp. 491–509.
3. F. F. LANGE, *Int. Met. Rev.* **1** (1980) 1.
4. M. H. LEWIS and R. J. LUMBY, *Powder Met.* **26** (1983) 73.
5. J. K. PATEL and D. P. THOMPSON, *Brit. Ceram. Trans. J.* **87** (1988) 70.
6. M. H. LEWIS and P. BANARD, *J. Mater. Sci.* **15** (1980) 443.
7. B. S. B. KARUNARATNE and M. H. LEWIS, *ibid.* **15** (1980) 449.
8. J. L. ISKOE, F. F. LANGE and E. S. DIAZ, *ibid.* **11** (1976) 908.
9. H. T. LARKER, in "Proceedings of the International Conference on HIP", edited by T. Garvare (CENTEK publishers, Luleå, 1988) pp. 19–26.
10. J. AUCOTE and S. R. FOSTER, *Mater. Sci. Technol.* **2** (1986) 700.
11. T. EKSTRÖM, *Mater. Sci. Engng* **A109** (1989) 341.
12. T. EKSTRÖM, L. K. L. FALK and E. M. KNUTSON-WEDEL, *J. Mater. Sci.* in press.
13. D. R. CLARKE, *J. Amer. Ceram. Soc.* **63** (1980) 104.
14. W. D. KINGERY, *J. Appl. Phys.* **30** (1959) 301.
15. I. A. AKSAY and J. A. PASK, *J. Amer. Ceram. Soc.* **58** (1975) 507.
16. W. WEISWEILER, *Sprechsaal* **114** (1981) 450.
17. N. A. TOROPOV, and I. A. BONDAR, *Izv. Akad. Nauk SSSR, Otd. Khim. Nouk* **4** (1961) 547.
18. I. A. BONDAR and F. J. GALAKHOV, *Izv. Akad. Nauk. SSSR, Ser. Khim.* **7** (1964) 1325.
19. P. DOERNER, L. J. GAUCKLER, H. KRIEG, H. L. LUKAS, G. PETZOW and J. WEISS, *Comput. Coupling Phase Diagrams Thermochem.* **3** (1979) 241–257.
20. N. A. TOROPOV, I. A. BONDAR, F. J. GALAKHOV, X. S. NIKOGOSYAN and N. V. VINOGRADOVA, *Izv. Akad. Nauk. SSSR, Ser. Khim.* **7** (1964) 1162.
21. G. CEVALES, *Ber. Deut. Keram. Ges.* **45** (1968) 217.
22. A. ROUANET, *Rev. Int. Hautes Temp. Refract.* **8** (1971) 161.
23. K. H. JACK, *Met. Technol.* **9** (1982) 297.
24. S. HAMPSHIRE, R. A. L. DREW and K. H. JACK, *Phys. Chem. Glasses* **26** (1985) 182.
25. R. A. L. DREW, S. HAMPSHIRE and K. H. JACK, in "Special Ceramics 7", edited by D. Taylor and P. Popper (British Ceramic Research Association, Stoke-on-Trent, 1981) pp. 119–132.

26. M. H. LEWIS, B. D. POWELL, P. DREW, R. J. LUMBY, B. NORTH and A. J. TAYLOR, *J. Mater. Sci.* **12** (1977) 61.
27. M. H. LEWIS, A. R. BHATTI, R. J. LUMBY and B. NORTH, *J. Mater. Sci.* **15** (1980) 103.
28. L. K. L. FALK, T. HERMANSSON and K. RUNDGREN, *J. Mater. Sci. Lett.* **8** (1989) 1032.
29. L. K. L. FALK and M. HOLMSTRÖM, in Proceedings of the 1st European Ceramic Society Conference, edited by G. de With, R. A. Terpstra and R. Metselaar (Elsevier Applied Science, London, 1989) pp. 1.373–1.377.
30. Y. CHENG and D. P. THOMPSON, *Brit. Ceram. Trans. J.* **87** (1988) 107.
31. F. F. LANGE, L. K. L. FALK and B. I. DAVIS, *J. Mater. Res.* **2** (1987) 66.
32. G. R. ANSTIS, P. CHANTIKUL, B. R. LAWN and D. B. MARSHALL, *J. Amer. Ceram. Soc.* **9** (1981) 553.
33. C. GRESKOVICH and G. E. GAZZA, *J. Mater. Sci. Lett.* **4** (1985) 195.
34. N. INGELSTRÖM and T. EKSTRÖM, in Proceedings of the International Conference on HIP, edited by T. Garvare (CENTEK publishers, Luleå, 1988) pp. 307–314.
35. G. ZIEGLER, J. HEINRICH and G. WÖTTING, *J. Mater. Sci.* **22** (1987) 3041.
36. F. F. LANGE, *ibid.* **17** (1982) 240.
37. A. V. VIRKAR and R. L. K. MATSUMOTO, in "Science and Technology of Zirconia III", edited by S. Somiya, N. Yamamoto and H. Yanagida (American Ceramic Society, Westerville, OH, 1988) pp. 653–662.

Received 22 June 1990
and accepted 31 January 1991